The Impact of Black Carbon Emissions from Projected Arctic Shipping on Regional Ice Transport

Xueke Li[1], Amanda H. Lynch[1,2], David A. Bailey[3], and Scott R. Stephenson[4]

[1]Institute at Brown for Environment and Society, Brown University, Providence, RI, USA.

[2]Department of Earth, Environmental and Planetary Sciences, Brown University, Providence, RI, USA.

[3]Climate and Global Dynamics Laboratory, National Center for Atmospheric Research, Boulder, CO, USA.

[4]RAND Corporation, Santa Monica, CA, USA.

Corresponding author: Xueke Li (xueke_li@brown.edu)

Key Points:

- Impact of black carbon emissions within-Arctic was quantified by re-routing 75% of shipping traffic from Suez Canal to Northern Sea Route
- Feedbacks were small Arctic-wide but amplified/dampened feedbacks were observed regionally primarily driven by a shift in circulation
- Largest feedback responses are distant from emission sources which has implications for good governance of expanding Arctic industries

Abstract

The direct and indirect effects of global emissions of black carbon (BC) on the evolution of Arctic climate has been well documented. The significance of within-Arctic emissions of BC is less certain. In light of this, an ensemble of scenarios are developed that simulate the hypothetical diversion of 75% of current and projected shipping traffic from the Suez Canal to the Northern Sea Route (NSR). This experiment shows that BC from ships results in a small change in climate forcing that does not influence the Arctic-wide trajectory of change. However, the shift in forcing from the Suez route to the NSR not only influences regional evolution of sea ice cover, but also results in regional feedbacks that in some locations amplify (e.g. Greenland Sea) and in other locations damp (e.g. Labrador Sea) the sea ice retreat under anthropogenic climate change. The primary mechanism underlying these regional effects is a shift in circulation rather than direct thermodynamic forcing. The most significant impacts are distal from the emissions sources, which is likely to have policy implications as the expansion of industrial and transportation activities into the Arctic is considered.

1 Introduction

Investors and communities alike are planning for the possible regime shift in Arctic shipping driven by receding ice, lower fuel prices, and industry consolidation [*Duarte et al.*, 2012; *Goldstein et al.*, 2018]. This shift has the potential, as yet unrealized, to make the transpolar shipping route at least seasonally competitive with the Suez Canal [*Buixadé Farré et al.*, 2014; *Meng et al.*, 2017; *Ng et al.*, 2018; *Theocharis et al.*, 2018]. Although the economic viability of transit shipping along such Arctic routes remains under considerable debate [*Hildebrand and Brigham*, 2018; *Lasserre*, 2014], ship traffic continues to increase due to Russian cabotage[1] [*Gunnarson*, 2013], fish stock migrations, and increased tourism [*Miller et al.*, 2020; *Stewart et al.*, 2007].

Black carbon (hereinafter referred to as BC) deposition on Arctic sea ice has been posited as one explanatory factor in observed rapid Arctic sea ice retreat [*Ramanathan and Carmichael*, 2008]. BC aerosols from sources including diesel engines, industrial processes and biomass burning absorb strongly across visible and ultraviolet wavelengths. As a result, it can influence Arctic temperatures and the extent of ice and snow cover by (i) directly absorbing solar radiation; (ii) acting as nuclei to form cloud drops and ice crystals, indirectly influencing cloud albedo via modifying the microphysical properties and lifetime of clouds [*Haywood and Boucher*, 2000; *Ramanathan and Carmichael*, 2008]; and (iii) reducing ice and snow albedo after deposition [*Flanner et al.*, 2009; *Ryan et al.*, 2018; *Warren*, 1982]. Previous studies suggest a measured decrease in Arctic albedo of 1.5 – 3.0% caused by snow and ice darkening from BC from all combustion sources, onshore and offshore [*Bond et al.*, 2013; *Hansen and Nazarenko*, 2004].

BC interactions and feedbacks are poorly constrained. For example, freshly emitted BC particles are generally hydrophobic and cannot serve as cloud condensation nuclei (CCN). Through microphysical aging processes, these carbonaceous particles gradually become hydrophilic on timescales that are highly variable [*Fierce et al.*, 2015]. These particles have a shorter average atmospheric residence time due to a high wet scavenging efficiency [*von*

[1] Cabotage in this paper, following *Gunnarsson* [2013], is defined as domestic port-to-port transport by both domestic and foreign carriers.

Schneidemesser et al., 2015]. The uncertainty in atmospheric residence time of BC is particularly evident in estimates of the distance from ship stacks to deposition. Given the complex web of uncertain processes, ranging from changes in albedo upon deposition, changes in snow metamorphism, phase partitioning in clouds, and cloud distribution properties, *Bond et al.* [2013] suggest that BC has an overall positive radiative forcing, accounting for direct and indirect effects, of +1.1 Wm^{-2} with 90% uncertainty bounds of +0.17 to +2.1 Wm^{-2}. The direct radiative effect, globally averaged for the industrial era, is estimated at +0.71 Wm^{-2} with 90% uncertainty bounds of +0.08 to +1.27 Wm^{-2}.

Maritime transport utilizing heavy fuel oil (HFO) contributes to BC emissions in the Arctic via incomplete combustion [*Corbett et al.*, 2010; *Wu et al.*, 2018]. Unlike BC transported to the Arctic from sub-Arctic terrestrial sources, BC emitted in the Arctic is more likely to remain at low altitudes, due to the typically strong surface inversion, particularly in the winter months. It has been posited that this has the potential to cause Arctic surface temperature to be nearly five times more sensitive to BC emitted within the Arctic than to emissions from lower latitudes, even though these emissions are much smaller in magnitude [*Sand et al.*, 2013a; *Sand et al.*, 2016]. It is unclear, however, how the frequency of surface inversions will change in the coming century [*Medeiros et al.*, 2011].

As a result of this potential sensitivity, studies have considered whether ship emissions of BC and other particulates will amplify or damp sea ice extent and snow cover feedbacks. Amplification of snow- and ice-albedo feedbacks can occur by deposition lowering the high albedo of ice and snow [*Browse et al.*, 2013; *Corbett et al.*, 2010; *Ødemark et al.*, 2012; *Sand et al.*, 2016]. Damping of these feedbacks can occur through indirect effects on clouds; for example, *Stephenson et al.* [2018] find an increase in the formation of clouds with high liquid water content could cause cooling relative to the shipping-free Arctic. All of these studies come with the caveat that BC emissions from Arctic shipping are small compared to those from the terrestrial sub-Arctic. These emissions may be reduced further in the context of a switch from HFO to low-sulfur diesel fuel or LNG and the reduced need for icebreakers, but this significance may increase as BC emissions from industry are reduced. Adding complexity to this issue, the use of low-sulphur fuels has been linked with a possible 85 percent increase in BC emissions [*DNV*, 2020]. We are seeking to understand the additional forcing of Arctic shipping-related BC, and in particular whether it constitutes a feedback of significance in the evolving system.

2 Data and methods

2.1 Climate Model Configuration

To quantify climate feedbacks of BC, we use the newly released Community Earth System Model version 2 (CESM2) at approximately 1° horizontal resolution with 32 vertical layers. CESM2 is a fully coupled earth system model that provides state-of-the-art simulations of climate. It contains seven prognostic model components (CAM6/WACCM6, CLM5, CISM2, POP2, CICE5, MOSART, and WW3) to comprehensively represent interactions among atmosphere, land, land-ice, ocean, and sea ice [*Danabasoglu et al.*, 2020].

CAM6 improves upon its previous version by including a unified turbulence scheme [*Golaz et al.*, 2002], adopting an updated Morrison-Gettelman cloud microphysics scheme (MG2) [*Gettelman and Morrison*, 2015], and applying a new scheme to calculate subgrid orographic drag [*Beljaars et al.*, 2004]. Notably, CAM6 treats aerosols using a four-mode

version of Modal Aerosol Model (MAM4) [*Liu et al.*, 2016]. That is, apart from Aitken, accumulation, and coarse modes preserved in the three-mode version (MAM3) [*Liu et al.*, 2012], an additional primary carbon mode is included in MAM4 to reside freshly emitted particulate organic matter (POM) and BC particles. This strategy allows for the conversion of particles from hydrophobic to hydrophilic. Compared to simulations with MAM3 that combine the primary carbon mode with the accumulation mode, which as a consequence, enhances wet removal of BC, the treatment of separating the primary carbon mode from the accumulation mode in MAM4 increases near-surface BC concentrations in the polar regions by a factor of 2 to 10 [*Liu et al.*, 2016].

In addition, the CESM large ensemble (CESM1-LENS, *Kay et al. 2015*) is used as a kind of proxy testbed [*Deser et al.*, 2020] to provide a more nuanced assessment of uncertainties arising from internal variability. The Large Ensemble Project provides 40 ensemble members performed with 1° resolution of fully-coupled CESM1 under RCP 8.5 from 2006-2100. As is standard practice, the slightly varying initial condition leads to an ensemble spread solely due to the model's internal climate variability [*Kay et al.*, 2015]. While this is not the model implementation used here, it can provide guidance as to the spread that might be expected in model responses in the present application. It should be noted that at the time of submission, all of the required variables from the CESM2 implementation of this large ensemble were not available.

2.2 Shipping emissions scenarios

Two sets of climate simulations with the CESM2 from 2015 to 2065 are performed. In the control experiment, projected monthly BC emissions from simulated trans-Arctic voyages are injected into the atmosphere along with BC emissions from *Peters et al.* [2011] and other emissions inventories from IPCC AR5 [*Lamarque et al.*, 2010] based on the Shared Socioeconomic Pathways (SSPs) 5 under the Representative Concentration Pathway (RCP) 8.5 scenario (*O'Neill et al.*, 2016, hereinafter referred to as SSP5-8.5). BC emitted from Arctic shipping is injected in the primary carbon mode of CAM6.

Small errors in the existing CMIP6 SSP5-8.5 scenario forcing (Figure 1(a)) were corrected to create a new control experiment rather than using the standard CMIP6 scenario. The main issues with the original SSP5-8.5 data are as follows. First, BC emissions in the standard scenario assume that the NSR is navigable all year round regardless of ice cover, when in reality, Arctic voyages are heavily concentrated in the peak months of July through October. We therefore limited shipping emissions to those months in which the NSR was technically accessible following the method of *Stephenson* et al. [2018], in order to reflect the seasonal cycle of Arctic shipping traffic. Second, there are interpolation artifacts in the standard scenario that are evident year round near the North Pole, which we have termed the "Santa Claus effect"; these were removed. Third, the HFO ban was implemented from 2020 in the standard scenario, but it is not yet in force. In October 2020, the IMO will vote on whether to approve a recommendation to ban the use and carriage of HFO in the Arctic by July 1, 2029 for Arctic country-flagged vessels operating in domestic waters, and by July 1, 2024 for all other voyages [*Humpert*, 2020]. Given that Russian vessels operating along the NSR are exempted from the shorter timeframe, approval by all Arctic states appears likely. Nevertheless, in the SSP5-8.5 forcing, the BC emissions are assumed to rise until 2020 and then begin to drop after this point, likely due to other treaties and not related to the HFO ban [*O'Neill et al.*, 2014]. To address this

complexity, the BC emissions in the new control simulation are modified as shown in Figure 1(b).

With the recent fall in oil prices, reasons to utilize the NSR for transit shipping have been less compelling in the near term. International transit shipping utilizing the entire NSR comprised less than 1% of all voyages from 2016-2018 [*B. Gunnarson, personal communication,* 2020]. These transits were primarily associated with demonstration voyages and the repositioning of vessels. In contrast, cabotage along the Russian Arctic coast comprised 88% of the total voyages on average over the same period, with monthly peaks of at least 250 voyages from July to October, and up to 400 voyages in September in some years. Thus, emissions associated with NSR transit shipping are a small fraction of the total BC load associated with Arctic shipping at present. Furthermore, the BC load in the Arctic is comprised primarily of sub-Arctic terrestrial sources [*Law and Stohl*, 2007; *Shindell et al.*, 2008]. In this uncertain context, to unambiguously characterize the climatic response to a postulated highly active route, a large perturbation was designed. The experiment is thus designated "big kick". Specifically, this approach lays the groundwork for understanding better what useful information might be gleaned from climate simulations of the impacts of NSR shipping in general, and where greater precision is likely to be most effective. In that spirit, an ensemble of integrations is conducted that re-routes 75% of BC emissions from current and projected Suez Canal traffic [*Gidden et al.*, 2019] to the Arctic, at equal 0.5-degree intervals along a route from the Bering Strait to Rotterdam (Figure 1(c)). Each of the ensemble members was performed with the "big kick" emissions, and a small perturbation to the surface air temperature to create internal variability. While four ensemble members is small, this should be sufficient to detect a signal in atmospheric circulation and sea ice responses, as described in *Deser et al.* [2012].

2.3 Quantifying feedback gain

An important target for this analysis is to reach an understanding of the potential for BC load to amplify or damp greenhouse gas feedback effects, as opposed to simply quantifying the additional forcing (both positive and negative) that BC imposes on the system. BC has potential for impacts that both amplify (through albedo reduction, *Hansen and Nazarenko,* 2004) and damp (through increases in cloud liquid water content, *Stephenson et al.*, 2018) the response to climate change. This is addressed through a feedback gain calculation following *Dufresne and Bony* [2008] based on the simple planetary energy balance response to a change in radiative forcing ΔR, viz.,

$$\Delta T = \frac{\Delta F_{TOA}^{rad} - \Delta R}{\lambda} \quad (1)$$

The total feedback effect can be divided into:

$$\lambda = \lambda_0 + \lambda_w + \lambda_{LR} + \lambda_c + \lambda_\alpha \quad (2)$$

where λ_0, λ_w, λ_{LR}, λ_c, and λ_α are feedback parameters of Planck, water vapor, lapse rate, cloud, and albedo, respectively. To this set, we add a hypothesized BC feedback parameter. Using this we can compare the basic equilibrium response to the observed temperature response, for example, by defining a feedback gain variable:

$$\Delta T = \frac{1}{1-g} \Delta T_E \quad (3)$$

in which $g = \sum_{x \neq 0} g_x$, and $g_x = -\frac{\lambda_x}{\lambda_0}$. Thus, we can calculate the feedback gain due to the change in BC forcing between the control and "big kick" experiments by

$$\Delta T_{65-15,"big\ kick"} = \frac{1}{1-g_{BC}} \Delta T_{65-15,control} \quad (4)$$

A similar procedure can be followed for ice volume and area. We acknowledge that our experiments are not in equilibrium, but nevertheless this is a useful measure that allows the integration of multiple interacting effects into a single metric. This serves to direct attention to more detailed analysis.

For analysis of the whole Arctic Ocean and its sub-regions, we define the Arctic following *Parkinson and Cavalieri* [2008] (thumbnail image shown in Figure 3(a)) with constituent sub-regions demarcating the Labrador Sea, the Greenland Sea, the Barents and Kara Seas, the Siberian Sea, the Beaufort Sea, the Central Arctic, the Arctic Ocean (including the Siberian Sea, the Beaufort Sea, and the Central Arctic, not shown), the Bering Sea, Seas of Okhotsk, the Canadian Archipelago, and Hudson Bay, abbreviated as Lab, GIN, Bar, Sib, Beau, CArc, ArcOc, Bering, Okhotsk, CAArch, and Hudson, respectively.

3 Whole Arctic Response

The total response to BC over the whole Arctic - ice volume, concentration, and distribution, surface temperature, broadband albedo, cloud fraction, longwave and shortwave heating rates - is modest, in line with previous studies [*Flanner*, 2013; *Holland et al.*, 2012; *Sand et al.*, 2013b]. These are not shown, since the significant differences (even at the 90% significance level) are very small. An indication of these differences is summarized in Table 1, in the form of linear trends for the last thirty years of the integrations (2035-2065) for the control experiment and the "big kick" ensemble mean. Based on these trends, it could be argued that the ice volume across the whole Arctic diminishes slightly more rapidly and the temperature increases slightly more in the ensemble mean compared to the control, as the presence of additional BC load in the atmosphere does result in the expected physical responses. But as is readily apparent, in the context of high interannual variability in this system, these results in aggregate are not statistically significant. More detail can be seen for example in Figure 2, which shows the time series of ice volume differences from each season, averaged across the ensemble members, expressed as a Z-score. This behavior is quite representative of individual ensemble member results in every season, and of other measures such as surface temperature and longwave heating rate. As is readily apparent, on an Arctic-wide basis, the rate of ice loss does not accelerate in the "big kick" experiment ensemble relative to the control. Thus, it is apparent that there is no net amplification (nor a damping) of the response that is sufficient to set up an additional feedback in the whole Arctic system.

This conclusion is reflected most efficiently in the calculation of the feedback gain parameter. In order to set bounds for significance in the feedback gain parameter, the CESM1-LENS ensemble members were compared pairwise (Figure 3(a)). The gain calculation is shown for the entire Arctic at the left of the figure, as well as being disaggregated into each the Arctic Seas. The median feedback for the whole Arctic is 0.00 with standard deviation of 0.21 for surface temperature, 0.21 for ice concentration and 0.20 for ice volume. The shading corresponds to the probability that the feedback gain magnitude would have been evident through internal system variability alone. This figure shows the potential for large feedback gain values evident

particularly in the Barents and Bering Seas generated by internal variability in the ensemble. Bringing the focus to the range more typical of the experiments being assessed here (Figure 3(b)) shows that - for the whole Arctic - the feedback gain in the "big kick" experiment cannot be considered to be significant for surface temperature, aggregate ice concentration or ice volume per unit area. As a result, it can be concluded that this experiment confirms previous research indicating that Arctic shipping, while having the potential to perhaps slightly influence the trajectory of Arctic sea ice retreat, does not induce additional Arctic-wide feedbacks.

4 Regional response

The same cannot be said, however, when disaggregating the response. Figure 3 also shows the feedback gain parameter for 11 distinct regions of the Arctic. The median feedback gain for the CESM1-LENS is zero for each of these regions. It is apparent that feedbacks are generated in the "big kick" ensemble in some of these regions at levels that amply exceed one standard deviation in the CESM1-LENS. While this cannot be a strict test of statistical significance, because of the different model configurations, it can serve as a guide to model responses that are likely to be outside of expectation from random chance.

The larger feedback gain values are negative in Baffin Bay and the Labrador and Siberian Seas, strongly positive in the Bering Sea, and somewhat positive in the GIN Seas and to a lesser extent the Barents/Kara Seas. The differing signs of the feedback gain in different regions suggest why the Arctic-wide feedback is effectively zero. That said, even though the median is zero, the variance in internally generated feedback gain in the CESM1-LENS is substantially greater than one in the Bering and Barents/Kara Seas, and as a result these two regions will be largely excluded from the following discussion.

It is particularly meaningful from a policy standpoint that the regions showing the largest "significant" feedback responses are distant from the regions where the additional BC load of the "big kick" experiment is largest (Figure 1). Furthermore, this suggests that the ice changes are influenced, if not driven, by perturbations in ice and atmosphere dynamical effects rather than albedo forcing by proximal deposition, or local cloud radiative forcing. This is borne out by, for example, a comparison of the longwave and shortwave heating rates in the GIN Seas (see supplementary Figure S1).

The sea level pressure (SLP) changes provide a useful indicator of atmospheric dynamical responses to the imposed BC load. The changes are modest but systematic, and may be summarized as a small but consistent tendency toward less negative indices for both the Northern Annular Mode and the Arctic dipole patterns (which can be diagnosed, for example, from the loadings onto EOF1 and 2 in the 1000hPa height fields, but are also apparent in the SLP patterns). This effect is in the context of an enhancement in the propensity toward a negative index Northern Annular Mode associated with greenhouse gas emissions that is typical of most climate change scenarios [*Gillett and Fyfe*; 2013]. These small shifts in the circulation that act as a perturbation on greenhouse gas forcing result in a reduction in the transpolar drift stream, a weakening of ice evacuation from the Siberian coast toward the Beaufort Sea, and a weakening of the ice exported out through the Bering Strait. All of these effects are consistent with the negative feedback gain parameter in the Siberian Sea and with findings such as those of *Wang et al.* [2009]. This is also consistent with the small but positive feedback gain in the aggregate ice area in the Beaufort Sea.

In the spring (MAM), there is also an eastward shift of the Siberian high associated with the Arctic Dipole (AD) in the ensemble mean "big kick" experiment (Figure 4). While the loading onto the AD mode varies across ensemble members, all members show an increasing propensity toward a positive mode in the last two decades of the simulations. This shift towards a slightly positive phase of AD has been demonstrated to lead to favorable conditions for enhanced ice export toward the Atlantic [*Watanabe et al.*, 2006].

In the summer (JJA), the SLP difference between the ensemble mean and the control reveals positive values centered on the western Arctic (that is, Iceland-Greenland-Canadian Archipelago-Beaufort Sea) and negative values centered on the eastern Arctic (Barents and Kara Seas-Laptev Sea-Siberian Sea). This feature is also evident in the results of *Overland et al.* [2012]. This persistent AD signature facilitates southerly wind flow from the Bering Strait, bringing warm North Pacific waters into the Arctic Ocean, but also accelerating ice export through Fram Strait [*Wang et al.*, 2009].

The signal in the North Atlantic is stronger, whereby the deepening of the polar low storm track in the GIN Seas is apparent, in all seasons, but particularly winter (DJF) and spring (MAM) (Figure 4). The impact on the ice regime in MAM is shown in Figure 5 for total, dynamic, ridging and thermodynamic ice differences from "big kick" ensemble member 1 for enhanced clarity (with the total MAM ice volume change for the other ensemble members shown in supplementary Figure S2). The overall impact in ice volume shows a redistribution from the eastern Barents and Kara Seas to the marginal ice zone in the GIN Seas. This is as a result particularly of the influence of dynamical processes as shown in the difference in ice volume due to ice transport and ridging (Figures 5(b) and (c)), although this is also reflected somewhat in the distribution of ice growth and melt (Figure 5(d)). An enhancement of the polar low storm track in all seasons apart from summer (JJA) leads to an increase in the incursion of sub-Arctic air into the region, with concomitant warming in the GIN and Barents Seas. Consistent with this logic are ice velocities that are generally more cyclonic in this region in the "big kick" ensemble members and increased ice drift speed in the region of enhanced export. As a result, significant changes in the ice regime are manifest all along the eastern Greenland coast even though this is distal from the perturbation in shipping activity.

The negative feedback gain parameters in the Baffin Bay and Labrador Sea region are also driven primarily by ice transport effects. This region, typical of Arctic projections, maintains a relatively heavy seasonal ice cover throughout much of the simulation across seasons, with spring (MAM) ice concentrations relatively flat at around 60% throughout the entire integration, even as the region is close to ice free in fall (SON). Ice thickness decreases in every season, and most rapidly in winter (DJF) and spring (MAM). Consistent signals across all ensemble members yielding statistically significant differences are also evident in warming temperatures and increased ice export from Baffin Bay out through the Labrador Sea. These changes in ice regime are then reflected in an increase in ice associated with thermodynamic growth. The conclusion based on these observations is that the modest additional warming evident in the "big kick" experiment is insufficient to offset the increased growth in ice as the shift in ice drift evacuates ice toward the south. A negative feedback then results in the western Greenland coastal zone.

This kind of integrative impact on ice cover associated with subtle shifts in circulation has been documented by *Kwok* [2000]; *Maslanik et al.* [2000]; and *Rigor et al.* [2002]. These dynamical mechanisms may also have profound implications for weather extremes in the mid-latitude [*Cohen et al.*, 2014; *Coumou et al.*, 2018].

5 Discussion

The future significance of international transit shipping in the Northern Sea Route will depend on numerous factors, including the interests and aspirations of Arctic nations, a sustainable cargo base, the length of the navigation season, and the availability of navigational support infrastructure. In this context, the effects of shipping on the climate system of the Arctic are small, but in our view, not insignificant.

The mitigation of black carbon emissions was expected to present "a potentially valuable opportunity with a very short delay between action and effect" [*Grieshop et al.*, 2009, p. 533]. This is particularly true for the Arctic due to the short time from emission to deposition (days to weeks [*Bond et al.*, 2013; *Hansen and Nazarenko*, 2004]). Our findings suggest this opportunity is more limited than might have been hoped. It is evident from these experiments and analyses that even a large perturbation in the usage of the Northern Sea Route, with its concomitant increase in black carbon emissions, is unlikely to be a significant factor in accelerating Arctic sea ice loss. Indeed, these simulations did not include the impacts of sulfate aerosols that attend enhancing shipping emissions, which can often yield a cooling effect [*Stephenson et al.*, 2018]. What is significant, however, is that these emissions do have the potential to affect regional feedback processes, that the mechanism underlying these effects is largely dynamical changes in the system, and that the most significant impacts are distal from the emissions themselves. Importantly, it appears that an important response is via the North Atlantic storm track, which has significance for operations in this busy region of the Arctic. As a result, policy-makers may have an interest in knowing more precisely what level of black carbon load, regardless of source, induces the observed regional changes.

Furthermore, the future of emissions contributions from Arctic ships - be they engaged in fishing, cabotage or transit - depends on the speed of technological developments and adoptions toward zero-emission fuels. The International Maritime Organization aims to halve emissions from shipping by 2050, while Arctic nations may adopt more ambitious targets in their sovereign seas. For example, the Norwegian Shipowners' Association has stated a goal of halving emissions by 2030, and to purchase only ships with zero-emissions technology from 2030. While these are relatively minor goals in the global black carbon budget, such aspirations form an important part of an overarching maritime shipping strategy.

Acknowledgments

This research was funded by the National Science Foundation through grant NNA/CNH-S 1824829: Modeling risk from variation in a coupled natural-human system at the Arctic ice edge. The authors appreciate the insightful discussions with Siri Veland and Michael Goldstein on the motivations for and relevance of these simulations for policy and communities. There are no conflicts of interest to report for any authors on this paper, not for the colleagues we acknowledge here. Previous and current CESM versions are freely available at www.cesm.ucar.edu:/models/cesm2/. Computing and data storage resources, including the Cheyenne supercomputer (doi:10.5065/D6RX99HX), were provided by the Computational and Information Systems Laboratory (CISL) at NCAR. The CESM datasets used in this study will be made available upon acceptance of the manuscript from the Earth System Grid Federation (ESGF) at esgf-node.llnl.gov/search/cmip6, or from the NCAR Digital Asset Services Hub (DASH) at data.ucar.edu.

References

Beljaars, A. C. M., A. R. Brown, and N. Wood (2004), A new parametrization of turbulent orographic form drag, *Quarterly Journal of the Royal Meteorological Society*, *130*(599), 1327-1347, doi:10.1256/qj.03.73.

Bond, T. C., et al. (2013), Bounding the role of black carbon in the climate system: A scientific assessment, *Journal of Geophysical Research: Atmospheres*, *118*(11), 5380-5552, doi:10.1002/jgrd.50171.

Browse, J., K. S. Carslaw, A. Schmidt, and J. J. Corbett (2013), Impact of future Arctic shipping on high-latitude black carbon deposition, *Geophysical Research Letters*, *40*(16), 4459-4463, doi:10.1002/grl.50876.

Buixadé Farré, A., et al. (2014), Commercial Arctic shipping through the Northeast Passage: routes, resources, governance, technology, and infrastructure, *Polar Geography*, *37*(4), 298-324, doi:10.1080/1088937X.2014.965769.

Cohen, J., et al. (2014), Recent Arctic amplification and extreme mid-latitude weather, *Nature Geoscience*, *7*(9), 627-637, doi:10.1038/ngeo2234.

Corbett, J. J., D. A. Lack, J. J. Winebrake, S. Harder, J. A. Silberman, and M. Gold (2010), Arctic shipping emissions inventories and future scenarios, *Atmos. Chem. Phys.*, *10*(19), 9689-9704, doi:10.5194/acp-10-9689-2010.

Coumou, D., G. Di Capua, S. Vavrus, L. Wang, and S. Wang (2018), The influence of Arctic amplification on mid-latitude summer circulation, *Nature Communications*, *9*(1), 2959, doi:10.1038/s41467-018-05256-8.

Danabasoglu, G., et al. (2020), The Community Earth System Model Version 2 (CESM2), *Journal of Advances in Modeling Earth Systems*, *12*(2), e2019MS001916, doi:10.1029/2019ms001916.

Deser, C., et al. (2020), Insights from Earth system model initial-condition large ensembles and future prospects, *Nature Climate Change*, *10*(4), 277-286, doi:10.1038/s41558-020-0731-2.

Deser, C., A. Phillips, V. Bourdette, and H. Teng (2012), Uncertainty in climate change projections: the role of internal variability, *Climate Dynamics*, *38*(3), 527-546, doi:10.1007/s00382-010-0977-x.

DNV, G. (2020), Initial results of a Black Carbon measurement campaign with emphasis on the impact of the fuel oil quality on Black Carbon emissions. Retrieved from https://www.euractiv.com/wp-content/uploads/sites/2/2020/01/PPR-7-8-Initial-results-of-a-Black-Carbon-measurement-campaign-with-emphasis-on-the-impact-of-the...-Finland-and-Germany.pdf.

Duarte, C. M., T. M. Lenton, P. Wadhams, and P. Wassmann (2012), Abrupt climate change in the Arctic, *Nature Climate Change*, *2*(2), 60-62, doi:10.1038/nclimate1386.

Dufresne, J.-L., and S. Bony (2008), An Assessment of the Primary Sources of Spread of Global Warming Estimates from Coupled Atmosphere–Ocean Models, *Journal of Climate*, *21*(19), 5135-5144, doi:10.1175/2008jcli2239.1.

Fierce, L., N. Riemer, and T. C. Bond (2015), Explaining variance in black carbon's aging timescale, *Atmos. Chem. Phys.*, *15*(6), 3173-3191, doi:10.5194/acp-15-3173-2015.

Flanner, M. G. (2013), Arctic climate sensitivity to local black carbon, *Journal of Geophysical Research: Atmospheres*, *118*(4), 1840-1851, doi:10.1002/jgrd.50176.

Flanner, M. G., C. S. Zender, P. G. Hess, N. M. Mahowald, T. H. Painter, V. Ramanathan, and P. J. Rasch (2009), Springtime warming and reduced snow cover from carbonaceous particles, *Atmos. Chem. Phys.*, *9*(7), 2481-2497, doi:10.5194/acp-9-2481-2009.

Gettelman, A., and H. Morrison (2015), Advanced Two-Moment Bulk Microphysics for Global Models. Part I: Off-Line Tests and Comparison with Other Schemes, *Journal of Climate*, *28*(3), 1268-1287, doi:10.1175/jcli-d-14-00102.1.

Gidden, M. J., et al. (2019), Global emissions pathways under different socioeconomic scenarios for use in CMIP6: a dataset of harmonized emissions trajectories through the end of the century, *Geosci. Model Dev.*, *12*(4), 1443-1475, doi:10.5194/gmd-12-1443-2019.

Gillett, N. P., and J. C. Fyfe (2013), Annular mode changes in the CMIP5 simulations, *Geophysical Research Letters*, *40*(6), 1189-1193, doi:10.1002/grl.50249.

Golaz, J.-C., V. E. Larson, and W. R. Cotton (2002), A PDF-Based Model for Boundary Layer Clouds. Part I: Method and Model Description, *Journal of the Atmospheric Sciences*, *59*(24), 3540-3551, doi:10.1175/1520-0469(2002)059<3540:apbmfb>2.0.co;2.

Goldstein, M. A., A. H. Lynch, A. Zsom, T. Arbetter, A. Chang, and F. Fetterer (2018), The step-like evolution of Arctic open water, *Scientific Reports*, *8*(1), 16902, doi:10.1038/s41598-018-35064-5.

Grieshop, A. P., C. C. O. Reynolds, M. Kandlikar, and H. Dowlatabadi (2009), A black-carbon mitigation wedge, *Nature Geoscience*, *2*(8), 533-534, doi:10.1038/ngeo595.

Gunnarson, B. (2013), The future of Arctic marine operations and shipping logistics, in *The Arctic in World Affairs: A North Pacific Dialogue on the Future of the Arctic, Proceedings of the North Pacific Arctic Conference (NPAC)*, edited by O.R. Young, J.-D. Kim, and Y.H. Kim, pp. 37–61, Korea Maritime Institute and East-West Center, Seoul and Honolulu.

Hansen, J., and L. Nazarenko (2004), Soot climate forcing via snow and ice albedos, *Proceedings of the National Academy of Sciences of the United States of America*, *101*(2), 423-428, doi:10.1073/pnas.2237157100.

Haywood, J., and O. Boucher (2000), Estimates of the direct and indirect radiative forcing due to tropospheric aerosols: A review, *Reviews of Geophysics*, *38*(4), 513-543, doi:10.1029/1999RG000078.

Hildebrand, L. P., and L. W. Brigham (2018), Navigating the Future: Towards Sustainable Arctic Marine Operations and Shipping in a Changing Arctic, in *Sustainable Shipping in a Changing Arctic*, edited by L. P. Hildebrand, L. W. Brigham and T. M. Johansson, pp. 429-435, Springer International Publishing, Cham, doi:10.1007/978-3-319-78425-0_23.

Holland, M. M., D. A. Bailey, B. P. Briegleb, B. Light, and E. Hunke (2012), Improved Sea Ice Shortwave Radiation Physics in CCSM4: The Impact of Melt Ponds and Aerosols on Arctic Sea Ice, *Journal of Climate*, *25*(5), 1413-1430, doi:10.1175/jcli-d-11-00078.1.

Humpert, M. (2020). IMO moves forward with ban of Arctic HFO but exempts some vessels until 2029. *High North News*, February 24. https://www.highnorthnews.com/en/imo-moves-forward-ban-arctic-hfo-exempts-some-vessels-until-2029

Kay, J. E., et al. (2015), The Community Earth System Model (CESM) Large Ensemble Project: A Community Resource for Studying Climate Change in the Presence of Internal Climate Variability, *Bulletin of the American Meteorological Society*, *96*(8), 1333-1349, doi:10.1175/bams-d-13-00255.1.

Kwok, R. (2000), Recent changes in Arctic Ocean sea ice motion associated with the North Atlantic Oscillation, *Geophysical Research Letters*, *27*(6), 775-778, doi:10.1029/1999gl002382.

Lamarque, J. F., et al. (2010), Historical (1850–2000) gridded anthropogenic and biomass burning emissions of reactive gases and aerosols: methodology and application, *Atmos. Chem. Phys.*, *10*(15), 7017-7039, doi:10.5194/acp-10-7017-2010.

Lasserre, F. (2014), Case studies of shipping along Arctic routes. Analysis and profitability perspectives for the container sector, *Transportation Research Part A: Policy and Practice*, *66*, 144-161, doi:https://doi.org/10.1016/j.tra.2014.05.005.

Law, K. S., and A. Stohl (2007), Arctic Air Pollution: Origins and Impacts, *Science*, *315*(5818), 1537-1540, doi:10.1126/science.1137695.

Liu, X., et al. (2012), Toward a minimal representation of aerosols in climate models: description and evaluation in the Community Atmosphere Model CAM5, *Geosci. Model Dev.*, *5*(3), 709-739, doi:10.5194/gmd-5-709-2012.

Liu, X., P. L. Ma, H. Wang, S. Tilmes, B. Singh, R. C. Easter, S. J. Ghan, and P. J. Rasch (2016), Description and evaluation of a new four-mode version of the Modal Aerosol Module (MAM4) within version 5.3 of the Community Atmosphere Model, *Geosci. Model Dev.*, *9*(2), 505-522, doi:10.5194/gmd-9-505-2016.

Maslanik, J. A., A. H. Lynch, M. C. Serreze, and W. Wu (2000), A Case Study of Regional Climate Anomalies in the Arctic: Performance Requirements for a Coupled Model, *Journal of Climate*, *13*(2), 383-401, doi:10.1175/1520-0442(2000)013<0383:acsorc>2.0.co;2.

Medeiros, B., C. Deser, R. A. Tomas, and J. E. Kay (2011), Arctic Inversion Strength in Climate Models, *Journal of Climate*, *24*(17), 4733-4740, doi:10.1175/2011jcli3968.1.

Meng, Q., Y. Zhang, and M. Xu (2017), Viability of transarctic shipping routes: a literature review from the navigational and commercial perspectives, *Maritime Policy & Management*, *44*(1), 16-41, doi:10.1080/03088839.2016.1231428.

Miller, L. B., J. C. Hallo, R. G. Dvorak, J. P. Fefer, B. A. Peterson, and M. T. J. Brownlee (2020), On the edge of the world: examining pro-environmental outcomes of last chance tourism in Kaktovik, Alaska, *Journal of Sustainable Tourism*, 1-20, doi:10.1080/09669582.2020.1720696.

Ng, A. K. Y., J. Andrews, D. Babb, Y. Lin, and A. Becker (2018), Implications of climate change for shipping: Opening the Arctic seas, *WIREs Climate Change*, *9*(2), e507, doi:10.1002/wcc.507.

O'Neill, B. C., et al. (2016), The Scenario Model Intercomparison Project (ScenarioMIP) for CMIP6, *Geosci. Model Dev.*, *9*(9), 3461-3482, doi:10.5194/gmd-9-3461-2016.

O'Neill, B. C., E. Kriegler, K. Riahi, K. L. Ebi, S. Hallegatte, T. R. Carter, R. Mathur, and D. P. van Vuuren (2014), A new scenario framework for climate change research: the concept of shared socioeconomic pathways, *Climatic Change*, *122*(3), 387-400, doi:10.1007/s10584-013-0905-2.

Ødemark, K., S. B. Dalsøren, B. H. Samset, T. K. Berntsen, J. S. Fuglestvedt, and G. Myhre (2012), Short-lived climate forcers from current shipping and petroleum activities in the Arctic, *Atmos. Chem. Phys.*, *12*(4), 1979-1993, doi:10.5194/acp-12-1979-2012.

Overland, J. E., J. A. Francis, E. Hanna, and M. Wang (2012), The recent shift in early summer Arctic atmospheric circulation, *Geophysical Research Letters*, *39*(19), doi:10.1029/2012gl053268.

Parkinson, C. L., and D. J. Cavalieri (2008), Arctic sea ice variability and trends, 1979–2006, *Journal of Geophysical Research: Oceans*, *113*(C7), doi:10.1029/2007jc004558.

Peters, G. P., T. B. Nilssen, L. Lindholt, M. S. Eide, S. Glomsrød, L. I. Eide, and J. S. Fuglestvedt (2011), Future emissions from shipping and petroleum activities in the Arctic, *Atmos. Chem. Phys.*, *11*(11), 5305-5320, doi:10.5194/acp-11-5305-2011.

Ramanathan, V., and G. Carmichael (2008), Global and regional climate changes due to black carbon, *Nature Geoscience*, *1*(4), 221-227, doi:10.1038/ngeo156.

Rigor, I. G., J. M. Wallace, and R. L. Colony (2002), Response of Sea Ice to the Arctic Oscillation, *Journal of Climate*, *15*(18), 2648-2663, doi:10.1175/1520-0442(2002)015<2648:rositt>2.0.co;2.

Ryan, J. C., A. Hubbard, M. Stibal, T. D. Irvine-Fynn, J. Cook, L. C. Smith, K. Cameron, and J. Box (2018), Dark zone of the Greenland Ice Sheet controlled by distributed biologically-active impurities, *Nature Communications*, *9*(1), 1065, doi:10.1038/s41467-018-03353-2.

Sand, M., T. K. Berntsen, J. E. Kay, J. F. Lamarque, Ø. Seland, and A. Kirkevåg (2013a), The Arctic response to remote and local forcing of black carbon, *Atmos. Chem. Phys.*, *13*(1), 211-224, doi:10.5194/acp-13-211-2013.

Sand, M., T. K. Berntsen, Ø. Seland, and J. E. Kristjánsson (2013b), Arctic surface temperature change to emissions of black carbon within Arctic or midlatitudes, *Journal of Geophysical Research: Atmospheres*, *118*(14), 7788-7798, doi:10.1002/jgrd.50613.

Sand, M., T. K. Berntsen, K. von Salzen, M. G. Flanner, J. Langner, and D. G. Victor (2016), Response of Arctic temperature to changes in emissions of short-lived climate forcers, *Nature Climate Change*, *6*(3), 286-289, doi:10.1038/nclimate2880.

Shindell, D. T., et al. (2008), A multi-model assessment of pollution transport to the Arctic, *Atmos. Chem. Phys.*, *8*(17), 5353-5372, doi:10.5194/acp-8-5353-2008.

Stephenson, S. R., W. Wang, C. S. Zender, H. Wang, S. J. Davis, and P. J. Rasch (2018), Climatic Responses to Future Trans-Arctic Shipping, *Geophysical Research Letters*, *45*(18), 9898-9908, doi:10.1029/2018gl078969.

Stewart, E. J., S. E. L. Howell, D. Draper, J. Yackel, and A. Tivy (2007), Sea Ice in Canada's Arctic: Implications for Cruise Tourism, *Arctic*, *60*(4), 370-380.

Theocharis, D., S. Pettit, V. S. Rodrigues, and J. Haider (2018), Arctic shipping: A systematic literature review of comparative studies, *Journal of Transport Geography*, *69*, 112-128, doi:https://doi.org/10.1016/j.jtrangeo.2018.04.010.

von Schneidemesser, E., et al. (2015), Chemistry and the Linkages between Air Quality and Climate Change, *Chemical Reviews*, *115*(10), 3856-3897, doi:10.1021/acs.chemrev.5b00089.

Wang, J., J. Zhang, E. Watanabe, M. Ikeda, K. Mizobata, J. E. Walsh, X. Bai, and B. Wu (2009), Is the Dipole Anomaly a major driver to record lows in Arctic summer sea ice extent?, *Geophysical Research Letters*, *36*(5), doi:10.1029/2008gl036706.

Warren, S. G. (1982), Optical properties of snow, *Reviews of Geophysics*, *20*(1), 67-89, doi:10.1029/RG020i001p00067.

Watanabe, E., J. Wang, A. Sumi, and H. Hasumi (2006), Arctic dipole anomaly and its contribution to sea ice export from the Arctic Ocean in the 20th century, *Geophysical Research Letters*, *33*(23), doi:10.1029/2006gl028112.

Wu, D., Q. Li, X. Ding, J. Sun, D. Li, H. Fu, M. Teich, X. Ye, and J. Chen (2018), Primary Particulate Matter Emitted from Heavy Fuel and Diesel Oil Combustion in a Typical Container Ship: Characteristics and Toxicity, *Environmental Science & Technology*, *52*(21), 12943-12951, doi:10.1021/acs.est.8b04471.

Table 1. Arctic wide average linear trend, per decade, 2035-2065, showing results from the control simulation, the ensemble mean and the standard deviation of the ensemble.

Figure 1. Global maps of BC anthropogenic emissions in February 2050 for (a) the standard SSP5-8.5 scenario forcing, (b) our modified forcing for the control simulation and (c) the emissions associated with the "big kick" ensemble.

Figure 2. Time series of ice volume difference between the "big kick" ensemble mean and the control simulation over the Arctic, expressed as a Z-score.

Figure 3. Response of BC in the Arctic and each subregion as defined by Parkinson and Cavalieri [2008] showing (a) the feedback gain parameter of the CESM1-LENS ensemble members selected pairwise (and a thumbnail map of the regions), and (b) a comparison between the CESM1-LENS ensemble members and the experiments. Shading of the CESM1-LENS results indicates the frequency of feedback gain value inferred from the probability density function, with darker colors implying higher frequency. The boxplot displays the median (white line) and interquartile range across four ensemble members of the "big kick" experiment.

Figure 4. Difference of sea level pressure between "big kick" ensemble mean and control for each season, defined by the months indicated, for the period 2035-2065.

Figure 5. Relative change in spring ice volume between "big kick" ensemble member 1 and control 2035-2065 by (a) total (b) dynamic (c) ridged and (d) thermodynamic processes. The relative change is computed using $(\text{Value}_{\text{"big kick"}} - \text{Value}_{\text{control}})/ \text{Value}_{\text{control}}$.

561
562

		Season			
		DJF	MAM	JJA	SON
Ice volume	Control	-0.008	-0.008	-0.008	-0.004
	"Big Kick"	-0.010 (0.003)	-0.009 (0.002)	-0.008 (0.002)	-0.005 (0.001)
Ice area	Control	-0.297	-0.106	-0.373	-0.515
	"Big Kick"	-0.358 (0.140)	-0.075 (0.070)	-0.383 (0.110)	-0.559 (0.119)
Albedo	Control	-0.001	0	0	-0.001
	"Big Kick"	-0.001 (0)	0 (0.0005)	0 (0)	0 (0.0005)
Surface temperature	Control	0.125	0.052	0.041	0.085
	"Big Kick"	0.156 (0.049)	0.058 (0.020)	0.043 (0.009)	0.088 (0.020)

563

564 Table 1.

565

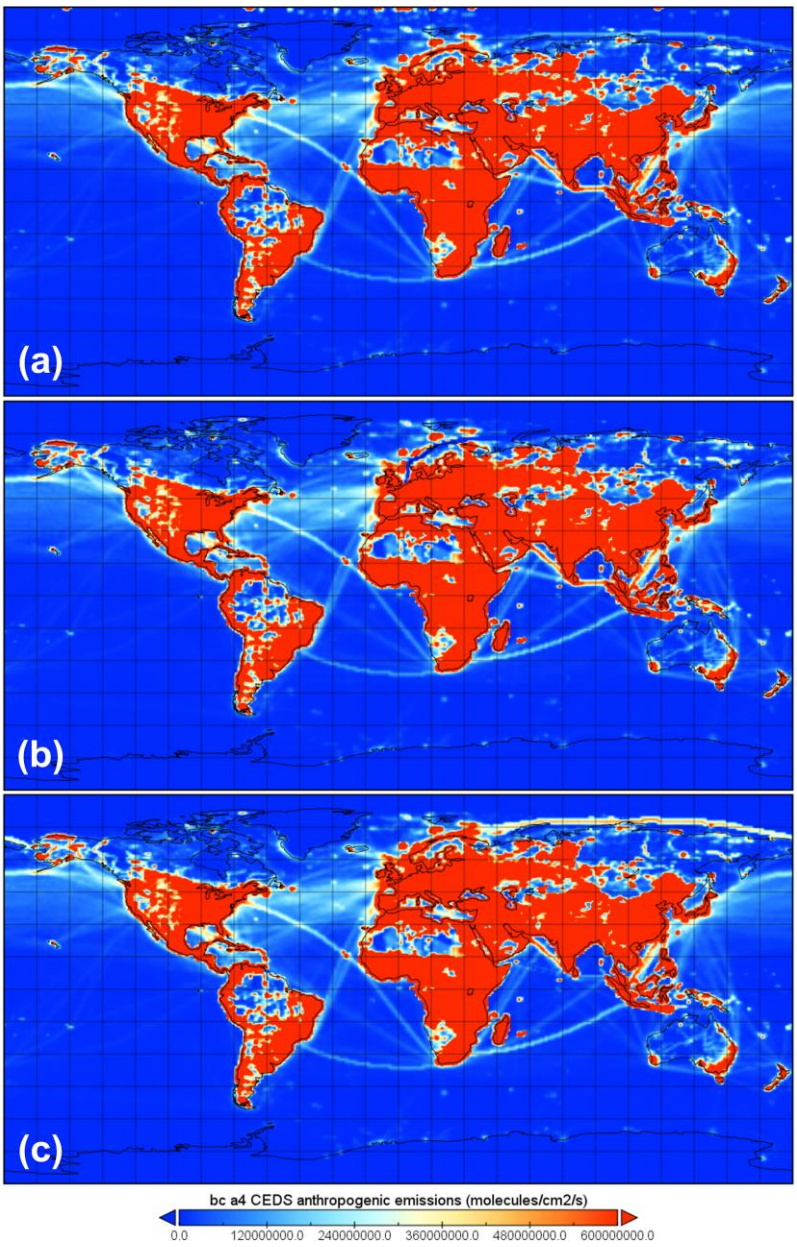
(a)
(b)
(c)
bc a4 CEDS anthropogenic emissions (molecules/cm2/s)
0.0
120000000.0
240000000.0
360000000.0
480000000.0
600000000.0

Figure 1.

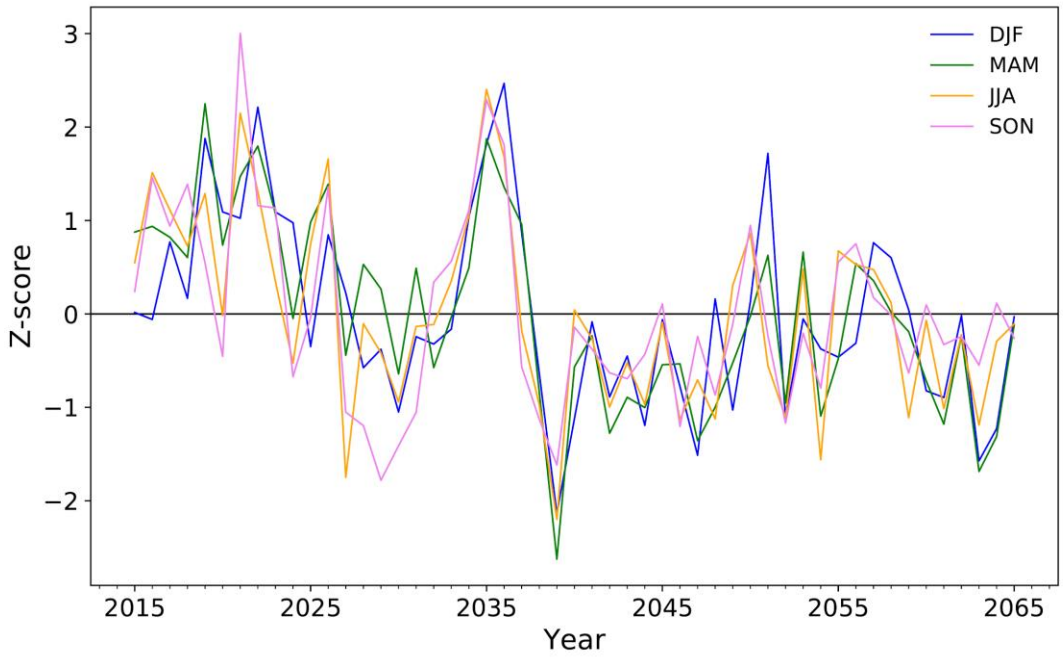
DJF
MAM
JJA
SON
Z-score
Year
3
2
1
0
−1
−2
2015
2025
2035
2045
2055
2065

Figure 2.

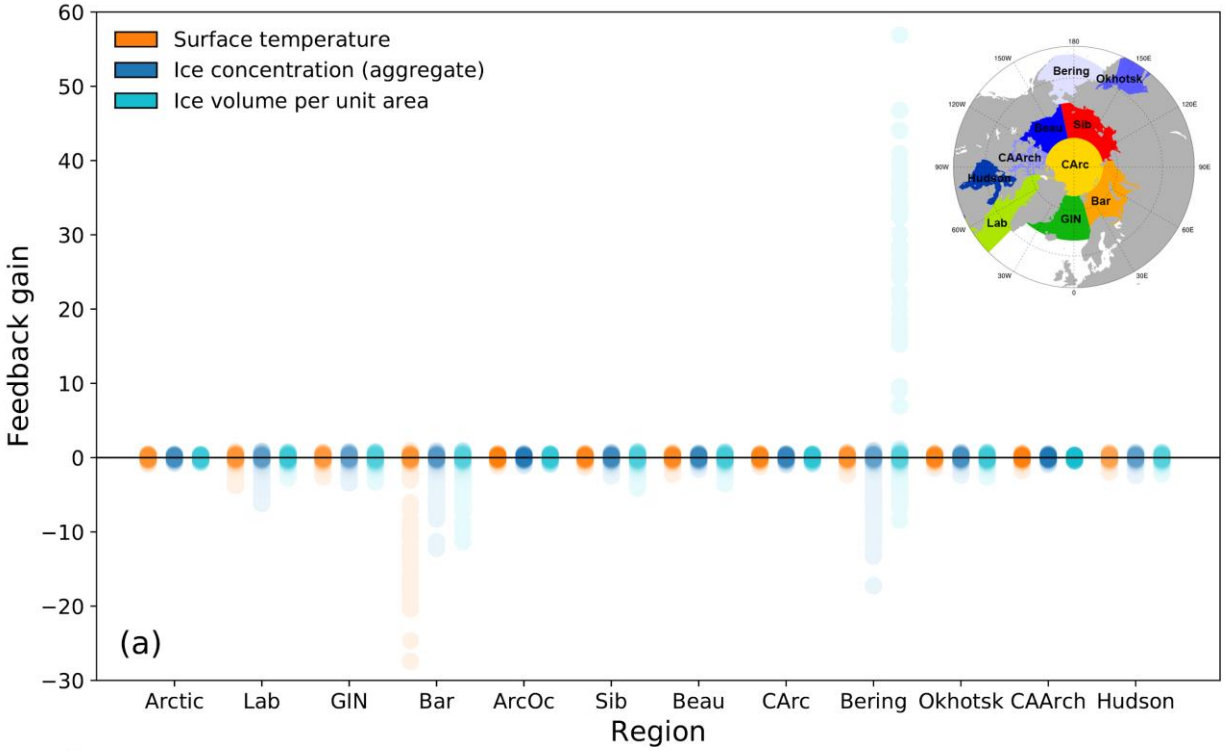
Surface temperature
Ice concentration (aggregate)
Ice volume per unit area
Feedback gain
(a)
Arctic
Lab
GIN
Bar
ArcOc
Sib
Beau
CArc
Bering
Okhotsk
CAArch
Hudson
Region
Bering
Okhotsk
Beau
Sib
CAArch
CArc
Hudson
Bar
Lab
GIN

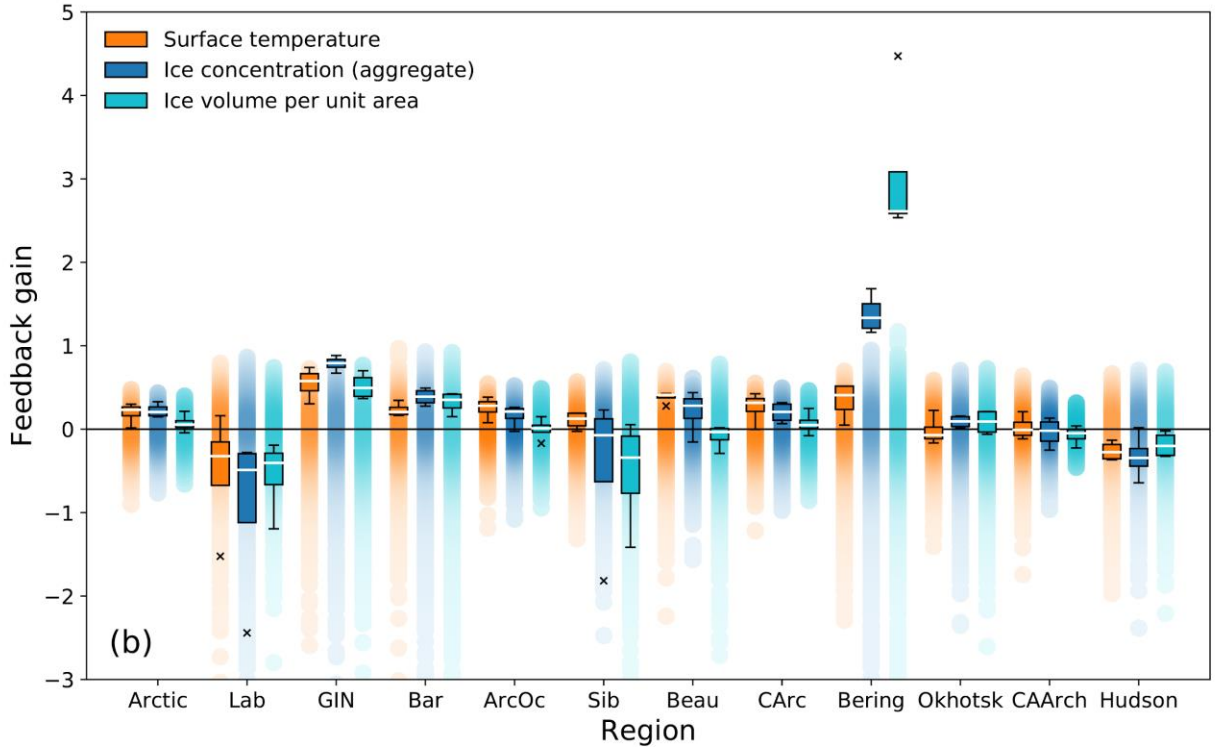
Surface temperature
Ice concentration (aggregate)
Ice volume per unit area
Feedback gain
(b)
Arctic
Lab
GIN
Bar
ArcOc
Sib
Beau
CArc
Bering
Okhotsk
CAArch
Hudson
Region

Figure 3.

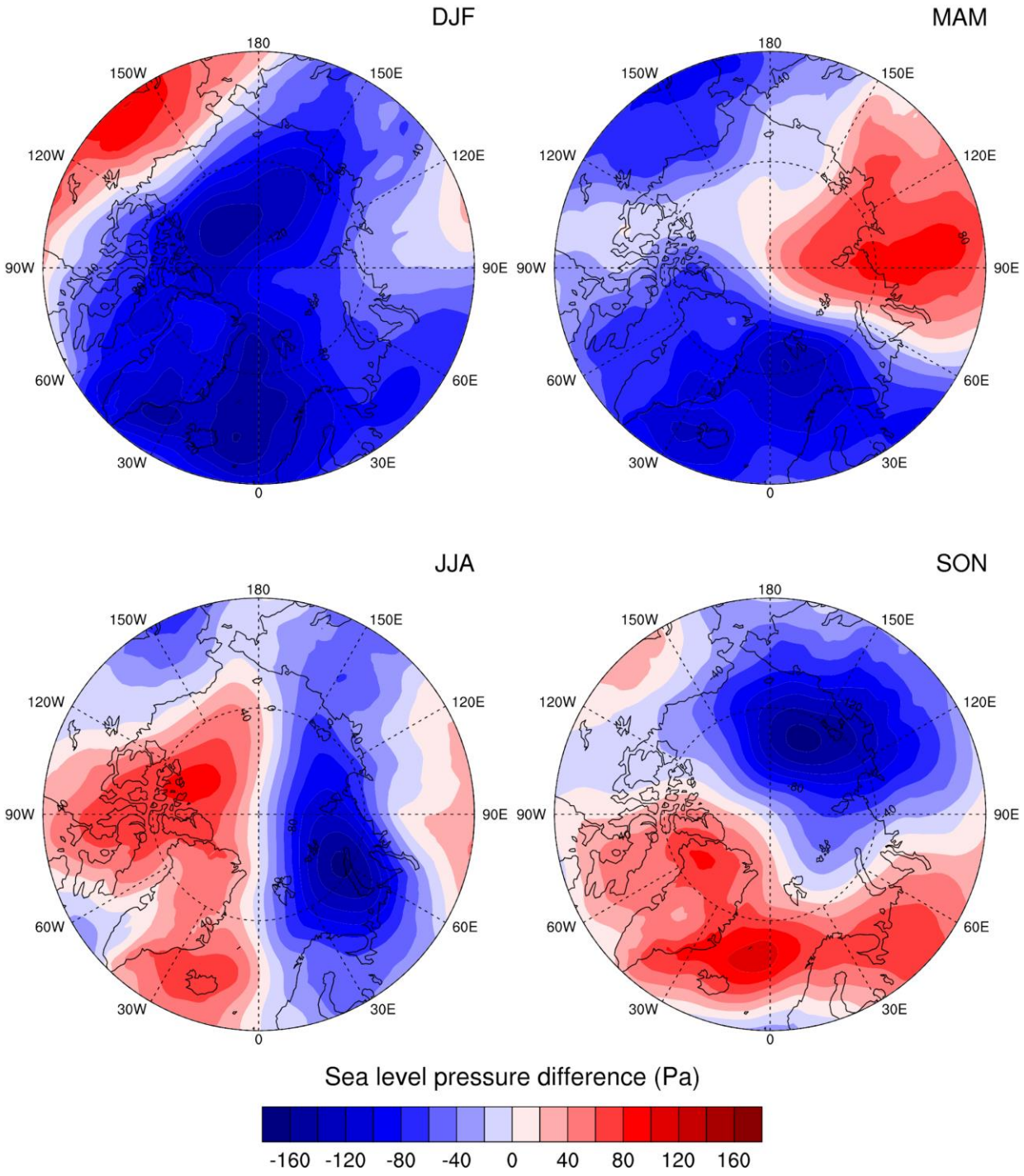
DJF
MAM
JJA
SON
180
150W
150E
120W
120E
90W
90E
60W
60E
30W
30E
0
Sea level pressure difference (Pa)
-160 -120 -80 -40 0 40 80 120 160

Figure 4.

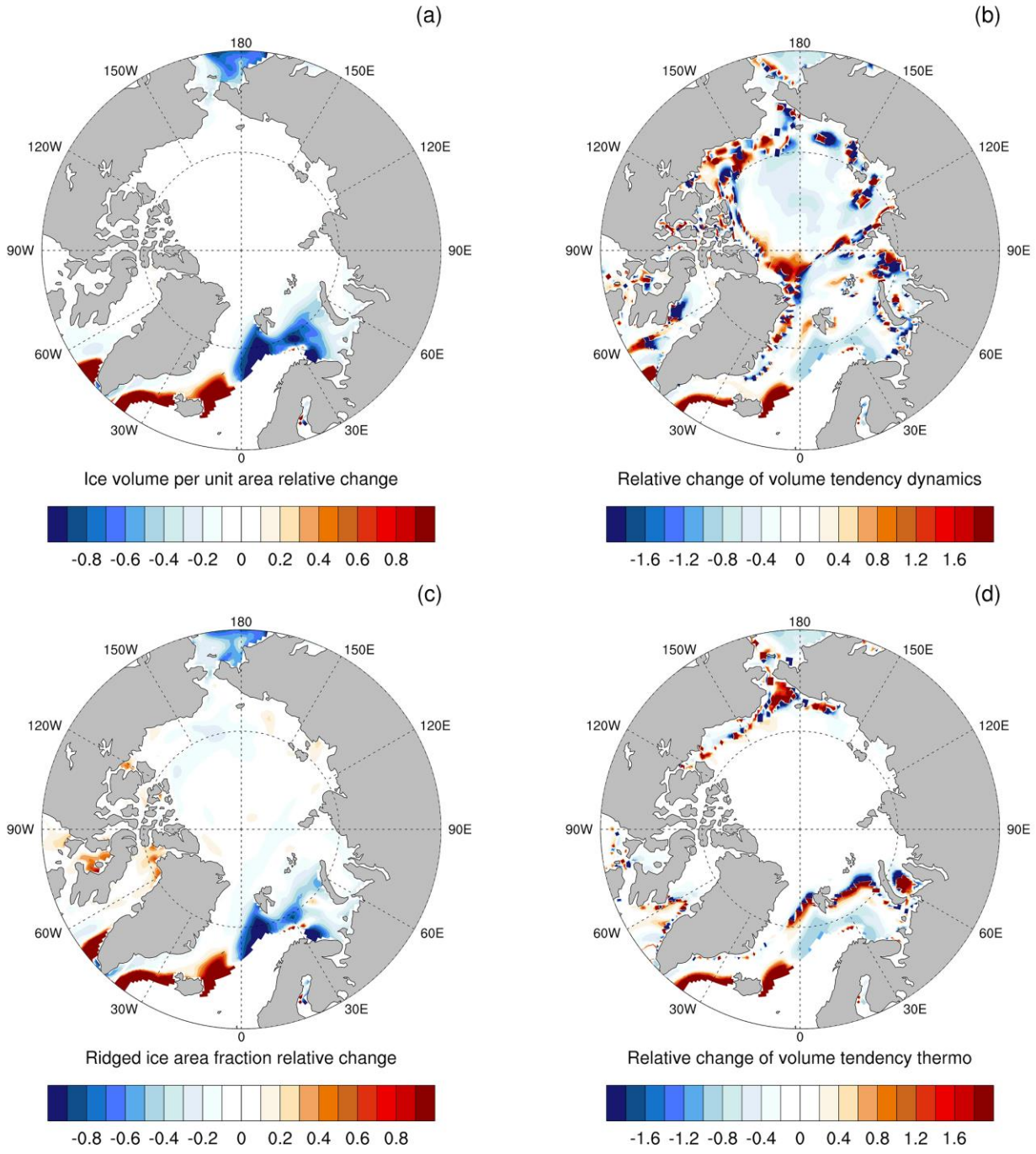
(a)
(b)
(c)
(d)
180
150W
150E
120W
120E
90W
90E
60W
60E
30W
30E
0
Ice volume per unit area relative change
Relative change of volume tendency dynamics
Ridged ice area fraction relative change
Relative change of volume tendency thermo
-0.8 -0.6 -0.4 -0.2 0 0.2 0.4 0.6 0.8
-1.6 -1.2 -0.8 -0.4 0 0.4 0.8 1.2 1.6

Figure 5.